Theor Chem Account (2007) 118:597–606
DOI 10.1007/s00214-007-0353-z

REGULAR ARTICLE

Non-alkane behavior of cyclopropane and its derivatives: characterization of unconventional hydrogen bond interactions

Annia Galano · J. Raúl Alvarez-Idaboy · Annik Vivier-Bunge

Received: 8 December 2006 / Accepted: 18 December 2006 / Published online: 7 June 2007

Abstract Eight cyclopropane derivatives ($\Delta - R$) have been modeled, with R = $-$H, $-$CH$_3$, $-$NH$_2$, $-$C $\equiv$ CH, $-$C $\equiv$ CCH$_3$, $-$OH, $-$F and $-$C $\equiv$ N. All geometries have been fully optimized at the MP2/ AUG-cc-pVTZ level of calculations. Natural bond orbital analyses reveal extra *p* character (sp^{λ}, $\lambda > 3$) in the C-C bonds of the cyclopropyl rings. The banana-like σ_{CC} bonds in the rings are described in detail. Alkene-like complexes between $\Delta - R$ molecules and hydrogen fluoride are identified. These weakly bonded complexes are formed through unconventional hydrogen bond interactions between the hydrogen atom in the HF molecule and the carbon–carbon bonds in the cyclopropane ring. A topological analysis of the electronic charge density and its Laplacian has been used to characterize the interactions. The possible relevance of such complexes in the modeling of substrate–receptor interactions in some anti-AIDS drugs is discussed.

Keywords Cyclopropane · Hybridization · Natural bond orbitals · Complex · Bonding · Alkene-like

Contribution to the Serafin Fraga Memorial Issue.

A. Galano (✉)
Instituto Mexicano del Petróleo, Eje Central Lázaro Cárdenas 152, 07730 México D. F., México
e-mail: agalano@imp.mx

J. R. Alvarez-Idaboy
Facultad de Química, Universidad Nacional Autónoma de México, Ciudad Universitaria, 04510 México D.F., México
e-mail: jidaboy@servidor.unam.mx

A. Vivier-Bunge
Área de Química Cuántica, Departamento de Química, Universidad Autónoma Metropolitana, Unidad Iztapalapa, México D.F., México

1 Introduction

Cyclopropane (C_3H_6, Δ) is an interesting molecule which represents a significant challenge to chemists. Considering that its C–C–C internuclear angles are 60°, it has anomalously low strain energy. It is also puzzling that its C–H bond vibrational frequencies resemble olefins much more closely than alkanes. Furthermore, cyclopropane undergoes addition reactions in a similar manner to ethylene [1]. Thus, it could be expected that this *alkene-like* behavior of cyclopropane might lead to the formation of unconventional hydrogen bonded complexes like those previously described for alkenes and aromatic compounds [2–5]. Since cyclopropane is present in the structure of many anti-AIDS drugs, such as nevirapine and efavirenz, and because hydrogen bonds are known to play a preponderant role in substrate–receptor interactions in biological systems, a detailed study of these complexes is relevant to the proper modeling of such systems.

Trying to understand and explain some of the unusual chemical properties of cyclopropane and its derivatives, and to describe the bonding scheme in a molecule with such acute bond angles, has occupied chemists for years [6–8]. Different theoretical treatments have been performed on cyclopropane. Walsh suggested that bonding results mainly from overlapping of three sp^2 hybrids (one on each carbon) pointing towards the center of the ring, i. e., a three-center two-electron bond [9]. This suggestion was confirmed by Hoffmann [10]. The "bent bond" model in cyclopropane was introduced by Coulson et al. [11–13]. Both theoretical and experimental studies [14–20] have shown that the electron distribution in the C–C internuclear region is not concentrated along the line between the nuclei, as in a typical covalent bond, but rather slightly outside this line.

Rozas et al. [21]. performed a theoretical study of the complexes formed between hydrogen fluoride and a series of

π-systems and cyclopropane. They concluded that an "unusual hydrogen bond" between the HF hydrogen atom and the π-cloud is responsible for the formation of the weakly bonded complexes.

On the other hand, Natural Bond Orbital (NBO) analysis [22–26] was originated as a technique for studying hybridization and covalency effects in polyatomic wave functions, based on local block eigenvectors of the one-particle density matrix. NBOs were conceived as a "chemist's basis set" that would correspond closely to the picture of localized bonds and lone pairs as basic units of molecular structure. Ab initio wave functions transformed to NBO form are found to be in good agreement with Lewis structure concepts and with the basic Pauling–Slater–Coulson picture [27,28] of bond hybridization and polarization. In orbital hybridization, as originally formulated by Pauling [27] and Slater [28], the sp^n hybrids of a central atom depend only on the number of ligands to be bonded. However, for nonequivalent ligands, and for unequal or highly strained bond angles, it is necessary to consider a more general sp^λ scheme, where λ is generally a non-integer (for more details see Ref. [22] and references there in). Accordingly, NBO analysis seems to be an excellent tool to describe the peculiarities of cyclopropane and its derivatives.

This work has two main goals. One of them is to quantitatively characterize the structure and bonding of cyclopropane derivatives. The second one, and probably the most relevant one, is to model their *alkene-like* behavior when they interact with polar species through unconventional hydrogen bonds. If our hypothesis is correct, and cyclopropyl groups are susceptible to form such bonds, the future modeling of several anti-AIDS drugs enzyme–inhibitor interactions should take them into account. We have modeled a series of $\Delta - R$ compounds, with $R = -\mathrm{H}, -\mathrm{CH_3}, -\mathrm{NH_2}, -\mathrm{C} \equiv \mathrm{CH}, -\mathrm{C} \equiv \mathrm{CCH_3}, -\mathrm{OH}, -\mathrm{C} \equiv \mathrm{N}$ and -F, and their complexes with an HF molecule. Those compounds with $R = -\mathrm{C} \equiv \mathrm{CH}$, and $-\mathrm{C} \equiv \mathrm{CCH_3}$ have been included in order to mimic the cyclopropane chemical environment in the drugs mentioned above. Topological analyses of the electronic charge density $\rho(r)$ and its Laplacian, $\nabla^2\rho(r)$, have also been performed in order to describe the characteristics of the interactions.

2 Computational details

A series of $\Delta - R$ compounds, with $R = -\mathrm{H}, -\mathrm{CH_3}, -\mathrm{NH_2}, -\mathrm{C} \equiv \mathrm{CH}, -\mathrm{C} \equiv \mathrm{CCH_3}, -\mathrm{OH}, -\mathrm{C} \equiv \mathrm{N}$ and -F, and their complexes with an HF molecule were modeled. Full geometry optimizations were performed with the Gaussian 98 [29] program using the ab-initio MP2 method and the Dunning's triple zeta correlation consistent basis sets [30,31] with diffuse functions (AUG-cc-pVTZ). MP2 stands for Hartree-Fock calculations followed by a M⊘ller–Plesset correlation energy correction [32], truncated at second order [33].

Frequency calculations were carried out for all the studied systems at the MP2/cc-pVTZ level of theory and minima were identified by the lack of imaginary frequencies (NIMAG = 0). Zero point energies (ZPE) and thermal corrections to the energy (TCE) at 298.15 K were included in the determination of the relative energies.

Natural bond orbital (NBO) analyses were performed using the NBO 3.1 program [34] as implemented in the Gaussian 98 package. In order to confirm the interactions leading to the complexes between Δ -it R compounds and the HF molecule, a Bader topological analysis [35] of the MP2/AUG-cc-pVTZ wave functions was also performed and several critical points were found. The topological analyses were computed with the Aim2000 program. [36,37]

3 Results and discussion

3.1 Geometries and molecular orbitals

The atoms' numbering used throughout this manuscript is shown in Fig. 1. Some geometrical parameters, corresponding to the optimized geometries are reported in Table 1. Additional modeling, at the same level of calculation, was also performed on ethene and ethane for comparison purposes. The C–C bond distances in the cyclopropyl ring are slightly shorter than in ethane and larger than in ethene. However, the C–H bond distances in the ring are very close to the corresponding distance in ethene. On the other hand, bond angles HCC have values of 111° and 117° for ethane and ethene, respectively, and the value for the cyclopropyl ring is closer to that of ethene. The same behavior is observed for the dihedral angle HCCH, which was found to be zero for all the studied cyclopropane derivatives.

To gain a better understanding of the electronic structure of $\Delta - R$ molecules, the molecular orbitals (MOs) were analyzed. Figure 2 shows some molecular orbitals with π-like character. These orbitals are close to the HOMO and partially localized above and below the C1–C2 bond, which suggests

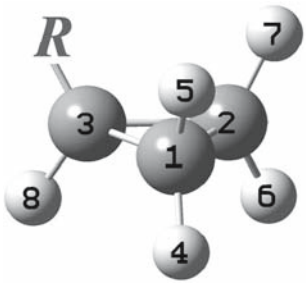

Fig. 1 Atoms numbering

Table 1 Geometrical parameters from the MP2/ AUG-cc-pVTZ optimized geometries

	Bond distances		Bond angles	
Ethane	CC	1.524	HCC	111.2
	CH	1.089	*HCH*	*107*.7
Ethene	CC	1.333	HCC	121.3
	CH	1.081	*HCH*	*117*.4
$\Delta - H$	C1C2	1.505	H4C1C2	117.7
	C1C3	1.505	H5C1C2	117.7
	C2C3	1.505	*H4C1H5*	115.1
	C1H4	1.079		
$\Delta - CH_3$	C1C2	1.510	H4C1C2	117.8
	C1C3	1.504	H5C1C2	117.4
	C2C3	1.504	*H4C1H5*	*115*.2
	C1H4	1.080		
$\Delta - NH_2$	C1C2	1.509	H4C1C2	118.2
	C1C3	1.501	H5C1C2	116.8
	C2C3	1.501	*H4C1H5*	*116*.1
	C1H4	1.079		
$\Delta - C \equiv CH$	C1C2	1.499	H4C1C2	118.2
	C1C3	1.515	H5C1C2	117.8
	C2C3	1.515	*H4C1H5*	115.9
	C1H4	1.079		
$\Delta - C \equiv CCH_3$	C1C2	1.500	H4C1C2	117.7
	C1C3	1.515	H5C1C2	118.1
	C2C3	1.515	*H4C1H5*	115.9
	C1H4	1.079		
$\Delta - OH$	C1C2	1.517	H4C1C2	118.6
	C1C3	1.500	H5C1C2	116.5
	C2C3	1.489	*H4C1H5*	*116*.1
	C1H4	1.079		
$\Delta - F$	C1C2	1.522	H4C1C2	119.0
	C1C3	1.487	H5C1C2	116.2
	C2C3	1.487	*H4C1H5*	*116*.1
	C1H4	1.079		
$\Delta - C \equiv N$	C1C2	1.497	H4C1C2	118.4
	C1C3	1.514	H5C1C2	117.8
	C2C3	1.514	*H4C1H5*	*115*.9
	C1H4	1.079		

that this bond could show a certain double-bond character. Their shapes resemble that of the ethylene's HOMO, which shows a nodal plane containing the C atoms. The orbitals in Fig. 2 show nodal surfaces involving the two carbon atoms with no substituents. Stable complexes were obtained between $\Delta - R$ and H–F molecules. Molecular orbitals with a clear bonding character between the fragments were found. Some of them are shown in Fig. 3. The ethylene system has been included for comparison.

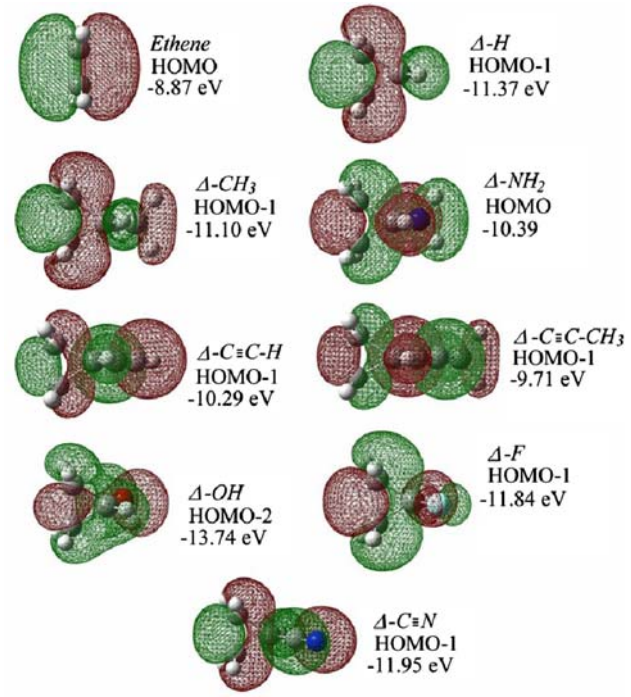

Fig. 2 π-like molecular orbitals in cyclopropane derivatives

As in the case of alkenes, the HF hydrogen atom points towards the C1–C2 bond. The fully optimized geometries of the complexes are displayed in Fig. 4, together with the equivalent complex between ethene and HF. They are formed through attractive interactions between the H atom in the hydrogen fluoride molecule and the center of the C1–C2 bonds. All the interaction distances were found to be in the vicinity of 2 Å, which is a typical hydrogen bond distance. They are similar to the ones previously described for alkene fragments with OH radicals [38–40] and water molecules [4,5]. The C1–C2 distances in the complexes (*cplx*) and their differences with respect to the corresponding free molecules (*fm*) are reported in Table 2. For all the studied systems, complex formation causes an elongation of the C1–C2 and H–F bond distances. The increase in the ethene C–C bond distance is very small (0.004 Å), while the increase in the C1–C2 bonds of the cyclopropane derivatives is found to be around 0.017 Åfor all the modeled systems.

3.2 Stabilization energies

The stabilization energies (E_{stab}) involved in the $\Delta - R$ + HF complex formation are reported in Table 3, together with the Gibbs free energy for the gas phase process. The values corresponding to the ethene + HF complex formation have also been included for comparison as well as the values corresponding to water dimer formation. This table shows the E_{stab} values without and with zero point energy

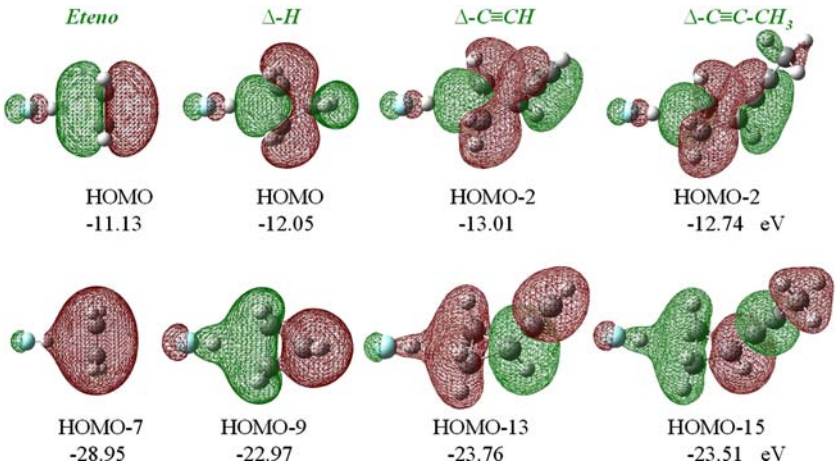

Fig. 3 Some of the molecular orbitals of the complexes, showing bonding character between fragments

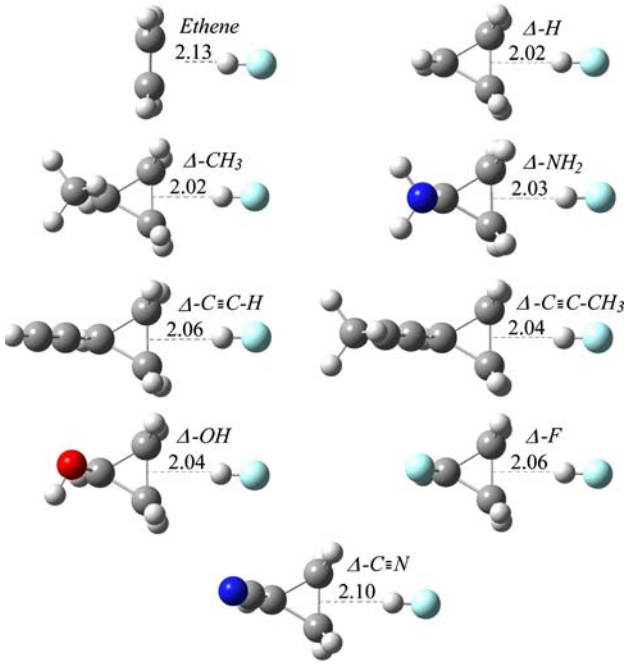

Fig. 4 MP2/AUG-cc-pVTZ fully optimized geometries of the $\Delta - R$ .. H–F complexes

Table 2 Relevant bond distances (Å) in the complexes (*cplx*), and their differences with respect to the corresponding free molecules (*fm*)

	d^{cplx}_{C1-C2}	d^{cplx}_{H-F}	$d^{cplx}_{C1-C2} - d^{fm}_{C1-C2}$	$d^{cplx}_{H-F} - d^{fm}_{H-F}$
Ethene	1.337	0.9318	0.004	0.0100
$\Delta - H$	1.522	0.9313	0.017	0.0095
$\Delta - CH_3$	1.527	0.9320	0.017	0.0102
$\Delta - NH_2$	1.526	0.9313	0.016	0.0095
$\Delta - C \equiv CH$	1.503	0.9295	0.017	0.0077
$\Delta - C \equiv CCH_3$	1.517	0.9305	0.017	0.0086
$\Delta - OH$	1.533	0.9305	0.016	0.0086
$\Delta - F$	1.538	0.9297	0.016	0.0079
$\Delta - C \equiv N$	1.513	0.9276	0.016	0.0057

corrections (ZPE) According to our results, electron donor groups increase the stability of the complexes, while electron withdrawing groups decrease it. In alkenes, unconventional hydrogen bonded complexes are stronger in propene than in ethene [39,40]. Also, positive inductive effects (+I) increase the alkenes reactivity towards electrophylic reagents. It can be seen that an analogous behavior is observed in the case of $\Delta - R \ldots H - F$ complexes: alkyl substitution on one carbon of the three members ring increases the tendency of cyclopropane derivatives to behave in an alkene-like way.

The stabilization energies involved in the interactions between an HF molecule with the modeled $\Delta - R$ were found to be slightly larger than the interaction with ethene for $R = -H$, $-CH_3$ and $-NH_2$. The compound closest in structure to the anti-AIDS drugs, $\Delta - C \equiv CCH_3$, also presents a large stabilization energy. In addition, these stabilization energies are of similar magnitude as the one corresponding to the water dimer formation ($E^{H2O}_{stab} = -5.18$ kcal/mol), at the same level of theory: MP2/ AUG-cc-pVTZ. Since the value for the water dimer is in excellent agreement with the experimental value (-5.4 ± 0.7 kcal/mol [41,42]), and taking into account the high level of theory employed, these results are expected to represent a correct description of the actual chemical behavior of the involved species. Interaction energies, as well as bond distances, are in the range of regular hydrogen bonds; therefore, they could be considered as non-conventional hydrogen bonds.

Since larger stabilization energies represent stronger interactions, it should be expected that the geometrical parameters described in the previous section reflect this feature. Accordingly, we have plotted the relation between E_{stab} and the H-F distance in the complexes in order to confirm our results. We have chosen the HF fragment because it remains the same in all the studied complexes. Figure 5 shows the expected

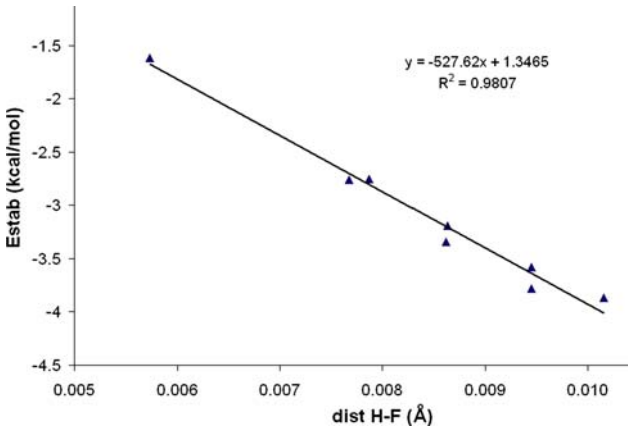

Fig. 5 Relationship between the H–F distance elongation and the stabilization energies

Table 3 Stabilization energies (E_{stab}, kcal/mol) and Gibbs free energy (ΔG) of $\Delta - R \ldots$ H-F complexes formation

	E_{stab}	E_{stab} (ZPE)	ΔG^{gas}
H_2O dimer	−5.18	−3.08	2.50
Ethene	−5.19	−3.24	3.01
$\Delta - H$	−5.16	−3.58	2.64
$\Delta - CH_3$	−5.40	−3.87	3.04
$\Delta - NH_2$	−5.25	−3.78	3.07
$\Delta - C \equiv CH$	−4.13	−2.76	4.00
$\Delta - C \equiv CCH_3$	−4.57	−3.19	3.62
$\Delta - OH$	−4.77	−3.34	3.46
$\Delta - F$	−4.11	−2.75	3.90
$\Delta - C \equiv N$	−2.77	−1.62	4.76

relationship: the larger the H–F distance in the complex, the stronger is the interaction.

As it can be seen in Table 3, the ΔG values corresponding to the complexes formation in gas phase are all positive, suggesting that they are non-viable processes. However, the value corresponding to the water dimer formation is also positive ($\Delta G^{gas} = 2.45$ kcal/mol), since this kind of complex is not expected to occur in the gas phase but in liquid one. Accordingly, it seems necessary to change the reference state a from 1atm to 1 M. Since K_P and K_C are related by

$$K_P = K_C (V_M)^{\Delta n}, \tag{1}$$

where V_M represents the molar volume and $\Delta n = -1$ for a bimolecular reaction, then

$$K_C = K_P V_M, \tag{2}$$

$$e^{-\frac{\Delta G^{1M}}{RT}} = e^{-\frac{\Delta G^{1atm}}{RT}} V_M \tag{3}$$

and from expression (3) it is evident that

$$\Delta G^{1M} = \Delta G^{1atm} - RT \ln (V_M). \tag{4}$$

Table 4 Gibbs free energies and equilibrium constants involved in the complexes formation in liquid phase

	ΔG^{1M}	ΔG^{1M+FV}	K_{eq}^{liq}
H_2O dimer	0.61	−1.93	2.60E+01
Ethene	0.75	−1.42	1.10E+01
$\Delta - H$	1.15	−1.79	2.06E+01
$\Delta - CH_3$	1.18	−1.39	1.04E+01
$\Delta - NH_2$	2.11	−1.36	9.86E+00
$\Delta - C \equiv CH$	1.73	−0.43	2.07E+00
$\Delta - C \equiv CCH_3$	1.57	−0.81	3.91E+00
$\Delta - OH$	2.01	−0.97	5.12E+00
$\Delta - F$	2.87	−0.53	2.44E+00
$\Delta - C \equiv N$	0.75	0.33	5.76E-01

This conversion lowers the ΔGs by 1.89 kcal/mol, for bimolecular reactions at 298 K. In addition, the free volume correction to liquid phase proposed by Benson [43] has also been included. According to this approach, the ratio between the reactions in solution and in gas phase, in nonpolar solvents, is

$$R \cong \frac{n 10^{(2n-2)}}{e^{(n-1)}}. \tag{5}$$

But, since the author previously assumed that

$$R \cong \frac{K_x^{sol}}{K_x^{gas}} \equiv \frac{e^{-\frac{\Delta G^{sol}}{RT}}}{e^{-\frac{\Delta G^{gas}}{RT}}}, \tag{6}$$

the combination of expressions (5) and (6) easily leads to

$$\Delta G^{sol} \cong \Delta G^{gas} - RT \left\{ \ln \left[n\, 10^{(2n-2)} \right] - (n-1) \right\}. \tag{7}$$

According to expression (7), ΔG^{sol} decreases by 2.54 kcal/mol for a bimolecular reaction ($n = 2$) at 298 K, with respect to ΔG^{gas}. Table 4 shows the ΔG values obtained for standard state of 1 M (ΔG^{1M}), and additionally including the Benson's free volume correction (ΔG^{1M+FV}). This approach has been successfully used before by Okuno [44] and Alvarez-Idaboy et al. [45] . It could be worthy to emphasize that this approach does not account for any direct interaction between the studied molecules and those of the solvent, but only for the solvent packing effects. However, this correction is necessary to avoid the overestimation of the entropy loss that arises from the complexes formation. In addition, this correction is general and applies to any solvent environment. In the same table, values of the corresponding equilibrium constant have been reported. It can be seen then for all systems the direct process, i.e, complexes formation, is favored ($K_{eq} > 1$), with the exception of $\Delta - C \equiv N$.

4 Topological analysis

The topological analysis of the electronic charge density $\rho(r)$ and its Laplacian, $\nabla^2\rho(r)$, is a powerful tool to describe the characteristics of bonds and interactions [19,35,46]. In particular, the critical points of $\rho(r)$, which present two negative curvatures and one positive curvature, identify the bonds in the molecule and will be denoted hereafter as bond critical points (BCP). The critical points with one negative and two positive curvatures are associated with the existence of a ring structure and will be denoted as ring critical points (RCP). The values of $\rho(r)$ and $\nabla^2\rho(r)$ at these points provide quantitative information on the strength and nature of the bonding and the characteristics of the ring. The Laplacian of the electronic charge density, $\nabla^2\rho(r)$, identifies regions of space wherein $\rho(r)$ is locally concentrated, $\nabla^2\rho(r) < 0$, or depleted, $\nabla^2\rho(r) > 0$. In general, negative values of $\nabla^2\rho(r)$ are typical of covalent interactions, whereas interactions between closed-shell systems are characterized by positive values of $\nabla^2\rho(r)$.

Topological analyses are very useful to characterize intermolecular interactions such as those described above between the HF molecule and the cyclopropane derivatives. Contour plots of the electron densities, obtained from the MP2/ AUG-cc-pVTZ wave functions of the modeled complexes are shown in Fig. 6. The complex between ethene and

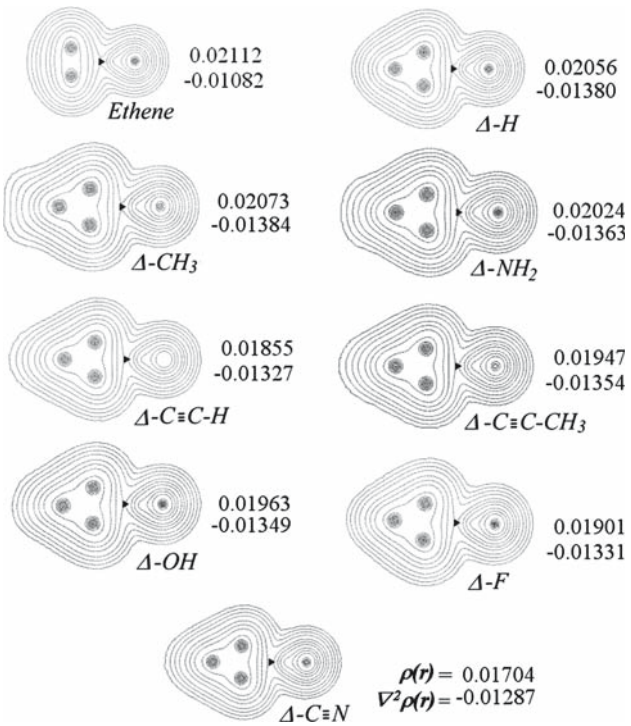

Fig. 6 Contour plots of the electron densities of the modeled complexes, from the MP2/ AUG-cc-pVTZ wave functions. (▲) indicates bond critical points associated with the HF ··· molecule interactions

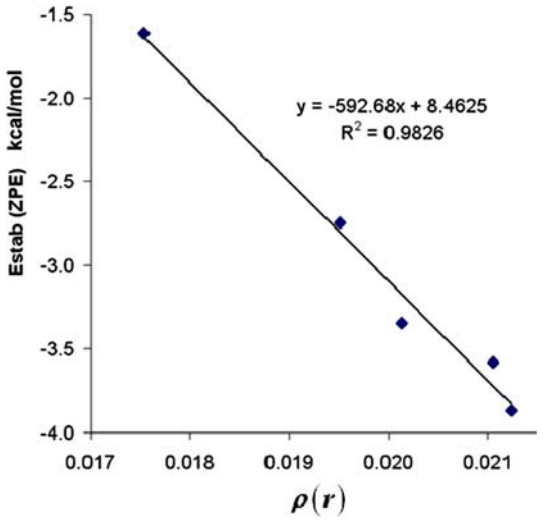

Fig. 7 Relationship between the charge density and the stabilization energies

HF has also been included for comparative purposes. In these plots, the bond critical points involved in the complexes formation have been marked as black triangles (▲). As can be observed in the figure, all the interactions are characterized by a bond critical point, confirming the existence of weak intermolecular hydrogen bond-like interaction between the pair fragments. It should be noticed that no ring critical point is observed; therefore, the weak bond is due to an interaction of the delocalized molecular orbitals of cyclopropane ring with the H atom of HF, i.e., the π-like molecular orbital is playing the role that is usually played by the p lone pair orbital of the donor. The values of $\rho(r)$ and $\nabla^2\rho(r)$, describing the interactions, have also been reported in Fig. 6.

It should be expected that a direct relationship exists between the charge density in the BCP that characterizes the interaction between the two fragments at the complex, and the corresponding stabilization energies. This tendency is shown in Fig. 7, Larger stabilization energies correspond to higher values of $\rho(r)$, since both represent stronger interactions.

4.1 Natural bond orbital analysis

To gain a better insight in to the peculiarities of the isopropyl derivatives we have additionally performed Natural bond orbital analyses. This approach comprises a sequence of transformations from the input basis set $\{\chi_i\}$ to various localized basis sets: natural atomic orbitals (NAOs), natural hybrid orbitals (NHOs), natural bond orbitals (NBOs) and natural localized molecular orbitals (NLMOs):

$$Inputbasis \rightarrow NAOs \rightarrow NHOs \rightarrow NBOs \rightarrow NLMOs$$

Table 5 Coefficients that characterize the σ_{C-C} bonds of the studied cyclopropand derivaties

		H	CH_3	NH_2	C ≡ CH	C ≡ CCH_3	OH	F	C ≡ N
σ_{C1-C2}									
	c_1	0.7071	0.7071	0.7071	0.7071	0.7071	0.7091	0.7071	0.7071
	λ_1	3.45	3.59	3.59	3.35	3.37	3.64	3.70	3.30
	c_2	0.7071	0.7071	0.7071	0.7071	0.7071	0.7051	0.7071	0.7071
	λ_2	3.45	3.59	3.59	3.35	3.37	3.68	3.70	3.30
σ_{C1-C3}									
	c_1	0.7071	0.7073	0.7052	0.6913	0.6938	0.7112	0.7109	0.6843
	λ_1	3.45	3.31	3.42	3.65	3.60	3.46	3.49	3.77
	c_3	0.7071	0.7069	0.7090	0.7226	0.7202	0.7030	0.7033	0.7292
	λ_3	3.45	3.63	3.45	3.69	3.69	3.19	3.04	3.58
σ_{C2-C3}									
	c_2	0.7071	0.7073	0.7052	0.6913	0.6938	0.7075	0.7109	0.6843
	λ_2	3.45	3.31	3.42	3.65	3.60	3.41	3.49	3.77
	c_3	0.7071	0.7069	0.7090	0.7226	0.7202	0.7067	0.7033	0.7292
	λ_3	3.45	3.63	3.45	3.69	3.69	3.23	3.04	3.58
σ^{a}_{C3-X9}									
	c_3	0.7703	0.7146	0.6411	0.7117	0.7107	0.5794	0.5222	0.7095
	λ_3	2.63	2.19	2.56	2.21	2.20	3.06	3.62	2.45
	x_9	0.6377	0.6996	0.7674	0.7025	0.7035	0.8151	0.8528	0.7047
	λ_9	*s*	2.35	2.07	1.08	1.09	2.26	2.47	0.90

[a] X stands for the atom in the R group directly bonded to C3

The localized sets may be subsequently transformed to delocalized natural orbitals (NOS) or canonical molecular orbitals (MOs). These steps are automated by the NBO computer programs. Each step of the sequence involves an orthonormal set that spans the full space of the input basis set and can be used to give an exact representation of the calculated wave function and of the average properties of the system.

The NBO for a localized σ bond between atoms A and B (σ_{AB}) is formed from directed orthonormal hybrids h_A, h_B (natural hybrid orbitals, NHOs):

$$\sigma_{AB} = c_A h_A + c_B h_B, \tag{8}$$

$$\sigma_{AB} = c_A \left(sp^{\lambda_A}\right)_A + c_B \left(sp^{\lambda_B}\right)_B \tag{9}$$

and the natural hybrids in turn are composed from a set of effective valence-shell atomic orbitals (natural atomic orbitals, NAOs) optimized for the chosen wave function.

For cyclopropane ($R = -$H), the localized σ_{C-C} bonds are identical and can be described by the symmetric NBOs:

$$\sigma_{C_1C_2} = \sigma_{C_1C_3} = \sigma_{C_2C_3} = 0.7071\left(sp^{3.45}\right) + 0.7071\left(sp^{3.45}\right).$$

The coefficients that characterize the σ_{C-C} bonds of the studied cyclopropane derivatives are reported in Table 5. An "extra" p character ($\lambda > 3$) is found for all the C–C bonds in the rings. This extra p character explains the alkene-like behavior observed in the reaction of cyclopropane derivatives reactions. Of course, this extra p-orbital character in the ring C–C bonds is achieved at the expense of a smaller p-orbital character in the exocyclic bonds. Table 5 also shows the polarization coefficients (c_A, c_B) and the hybridization coefficients (λ_A, λ_B) corresponding to the C3–X9 bond in the R group directly bonded to C3, where X represents the atom in the R group directly bonded to one of the C atoms in the cyclopropyl ring. Large polarization coefficients indicate high electronegativities. Accordingly, while the values of c_A and c_B corresponding to the σ_{CC} bonds in the rings are very similar; there is a noticeable difference between the pair of polarization coefficients associated with the σ_{C3X9} bonds. There also seems to be a relationship between the electronegativity of X9 and the λ value corresponding to C3 in the σ_{C3X9} bond. The larger the electronegativity of X9 (c_9), compared to that of the C3 atom (c_3), the larger is the hybridization coefficient of C3 (λ_3) in the σ_{C3X9} bond.

NBO analysis also yields information on the direction of the natural hybrid orbitals. Deviations from the line of nuclear centers are used to show the changes in the directions of natural hybrid orbitals, i.e., the *bond bendings*. Since the bonds in the cyclopropane rings are often described as *banana-like*, we report the bending angle (in degrees) of the bonds with respect to a line between the nuclei, both in $\Delta - R$ and in the complexes formed through interactions between the HF molecule and the cyclopropyl rings (Table 6). The deviation values corresponding to the bonds involved in the complexes formation have also been included in the table, and it

Table 6 Deviation angles of the NHO bonds (in degrees) with respect to a line between nuclear centers in the free $\Delta - R$ molecule (*fm*) and in the $\Delta - R \cdots$ HF complexes (*cplx*)

NHO		H	CH_3	NH_2	C_2H	C_2CH_3	OH	F	CN
$h_{C_1}(\sigma_{C_1C_2})$	*fm*	24.3	25.0	23.7	23.2	22.7	23.9	24.3	22.9
	cplx	25.7	25.2	25.2	24.9	24.5	25.4	25.7	24.7
$h_{C_2}(\sigma_{C_1C_2})$	*fm*	24.3	25.0	23.7	23.2	22.7	24.0	24.3	22.9
	cplx	25.7	25.2	25.2	24.9	24.5	25.5	25.7	24.7
$h_{C_1}(\sigma_{C_1C_3})$	*fm*	24.3	23.8	22.8	22.6	22.1	23.2	22.7	22.0
	cplx	22.1	23.1	22.3	22.7	22.5	25.4	22.1	22.4
$h_{C_3}(\sigma_{C_1C_3})$	*fm*	24.3	23.0	24.2	22.8	23.0	25.2	25.1	22.8
	cplx	23.0	22.4	22.8	22.2	21.8	25.5	23.0	22.3
$h_{C_2}(\sigma_{C_2C_3})$	*fm*	24.3	23.8	22.8	22.6	22.1	22.3	22.7	22.0
	cplx	22.1	23.1	22.3	22.7	22.5	21.8	22.1	22.4
$h_{C_3}(\sigma_{C_2C_3})$	*fm*	24.3	23.0	24.2	22.8	23.0	24.2	25.1	22.8
	cplx	23.0	22.4	22.8	22.2	21.8	22.0	23.0	22.3

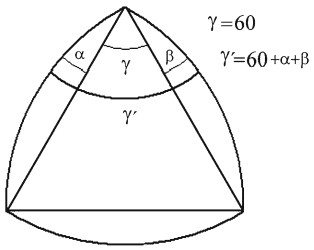

Fig. 8 Schematic representation of nuclear centered and deviated bonds

Table 7 γ' values corresponding to the studied $\Delta - R$ molecules

R=	H	CH_3	NH_2	C_2H	C_2CH_3	OH	F	CN
C2**C1**C3	108.6	108.8	106.5	105.8	104.8	107.1	107.0	104.9
C1**C2**C3	108.6	108.8	106.5	105.8	104.8	106.3	107.0	104.9
C2**C3**C1	108.6	106.0	108.4	105.6	106.0	109.4	110.2	105.6

can be noticed that bending corresponding to C1–C2 bonds increases when in the complexes, compared to the free molecules, which is an expected consequence of the interaction with the HF molecule.

It is well known that in acyclic molecules tetrahedral angles of 109° between sp^3 hybridized carbons are preferred, while in the cyclopropyl rings these angles are about 60°, leading to ring strain. However, the angle deviations reported above help the cyclopropyl rings to overcome some of the strain. If the carbon-carbon σ bonds are not localized along the internuclear axis, but are rather bent outwards from the line of nuclear centers, then a bond angle much wider than 60° can be achieved (Fig. 8). Let us use the C_6H_6 molecule as an example. In this case $\gamma = 60^o, \alpha = 24.3^o$ and $\beta = 24.3^o$. Therefore, $\gamma' = 108.3^o$, which is very close to the ideal value of 109° . The γ' values corresponding to all the studied cyclopropane derivatives are reported in Table 7. These values provide an explanation for the anomalously low strain energy of cyclopropane.

4.2 Relevance in anti-AIDS drug modeling

The magnitude of the stabilization energy arising from the complexes formation is about 3 kcal/mol, except when *R* groups are highly withdrawing. This value represents about 25% of the substrate–receptor interaction energy of anti-AIDS drugs containing cyclopropyl groups, which ranges from −8 to −11 kcal/mol. Thus, they could be relevant to HIV inhibition. To the best of our knowledge, this kind of interaction has not been considered in previous structure-activity modeling [47–49].

In a recent experimental work on efavirenz [50] and phenylethylthiazolthiourea (urea-PETT) [51] analogues, the influence of cyclopropyl groups on the antiviral activity of these drugs was studied. Högberg et al. [51] concluded that cyclopropane urea analogues are more potent than ethyl-linked urea compounds. Cocuzza et al. [50] studied two series of efavirenz derivatives: one in which the cyclopropane ring was replaced by small heterocycles, and another one in which the whole acetylenic side chain was replaced. According to their results, compounds in the first series retain most of their antiviral activity, but it is slightly smaller than that of efavirenz. For the compounds on the second series, the authors reported that unsaturated compounds are the most active. However, they are all less active than efavirenz, except for the $-CH_2CH = C(CH_3)_2$ analogue. Interestingly enough, this is a non-polar fragment capable of forming unconventional hydrogen bonds.

This experimental evidence, together with the data reported in this work, suggest that unconventional hydrogen bond interactions could play an important role in the antiviral

activity of these drugs. Consequently, future modeling of their structure–activity relationship should include the cyclopropyl interactions described here.

5 Conclusions

Eight cyclopropane derivatives ($\Delta - R$) have been modeled, with R $= -$H, $-CH_3$, $-NH_2$, $-C \equiv CH$, $-C \equiv CCH_3$, $-$OH, $-$F and $-C \equiv$ N. Their geometries have been fully optimized at the MP2/ AUG-cc-pVTZ level of calculations. The cyclopropane derivatives and complexes were additionally characterized by topological and natural bond orbital analyses. The latter reveal extra p character (sp^{λ}, $\lambda > 3$) in all the C–C bonds in the cyclopropyl rings. Moreover,Our calculations indicate that polar molecules can interact with cyclopropane and its derivatives in a manner that is similar to the one in alkenes. Weakly bound complexes are found, with geometries that resemble those typical of alkenes. Stabilization energies that are larger than the one for the ethene $\cdots$ HF complex are obtained for R $= -$H, $-CH_3$ and $-NH_2$.

The unconventional hydrogen bond interactions between $\Delta - R$ and an HF molecule may be relevant to the full understanding of different chemical processes, not only related to organic chemistry but also to biological processes, where polar molecules are susceptible to interact on with molecular fragments containing cyclopropane rings, such as some anti-AIDS drugs. According to our results, the possible formation of unconventional hydrogen bond interactions may be essential in structure–activity studies of systems containing a cyclopropane ring.

Acknowledgements The authors thank the IMP Computing Center for supercomputer time on SGI Origin 3000. This work was partially supported by Grant DGAPA UNAM (PAPIIT-IN203206-2), Mexico the SEP-CONACYT Project SEP-2004-C01-46167 and PROMEP through a grant to establish the "Quantum Chemistry and Molecular Simulation" network.

References

1. Cromwell NH, Graff MA (1952) J Org Chem 17:414
2. Oku K, Watanabe H, Kubota M, Fukuda S, Kurimoto M, Tsujisaka Y, Komori M, Inoue Y, Sakurai M (2003) J Am Chem Soc 125:12739
3. Tarakeshwar P, Choi HS, Lee SJ, Lee JY, Kim KS, Ha TK, Jang JH, Lee JG, Lee H (1999) J Chem Phys 111:5838
4. Tarakeshwar P, Kim KS, Brutschy B (2000) J Chem Phys 112:1769
5. DuPré DB, Yappert MC (2002) J Phys Chem A 106:567
6. Ferguson LN (1973) Highlights of alicyclic chemistry. Franklin, Palisades
7. Roberts JD, Caserio MC (1977) Basic principles of organic chemistry, 2nd ed. Benjamin, Menlo Park, (1983)
8. Morrison RT, Boyd RN (1983) Organic chemistry, 4th edn. Allyn and Bacon, Boston
9. Walsh AD (1949) Trans Faraday Soc 45:179
10. Hoffmann R (1964) J Chem Phys 40:2480
11. Coulson CA, Moffitt WE (1949) Philos Mag 40:1
12. Coulson CA, Googwin TH (1963) J Chem Soc 2851:3161
13. Walsh AD (1949) Trans Faraday Soc 45:179
14. Fritchie CJ Jr (1966) Acta Crystallogr 20:27
15. Hartman A, Hirshfeld FL (1966) Acta Crystallogr. 20:80
16. Stevens RM, Switkes E, Laws EA, Lipscomb WN (1971) J Am Chem Soc 93:2603
17. Ito T, Sakurai T (1973) Acta Crystallogr Sect B 29:1594
18. Bader RWF, Nguyen-Dang TT (1981) Adv Quantum Chem 14:63
19. Bader RWF, Tang TH, Tal Y, Biegler-Konig FW (1982) J Am Chem Soc 104:940
20. Politzer P (1983) Chem Phys Lett 102:74
21. Rozas I, Alkorta I, Elguero J (1997) J Phys Chem A 101:9457
22. Foster JP, Weinhold F (1980) J Amer Chem Soc 102:7211
23. Reed AE, Weinhold F (1983) J Chem Phys 78:4066
24. Reed AE, Weinhold F (1983) J Chem Phys 78:1736
25. Reed AE, Weinstock RB, Weinhold F (1985) J Chem Phys 83:735
26. Reed AE, Curtiss LA, Weinhold F (1988) Chem Rev 88:899
27. Pauling L (1931) J Am Chem Soc 53:1367
28. Slater J (1931) C Phys Rev 37:481
29. Gaussian 98, Revision A3, Frisch MJ, Trucks GW, Schlegel HB, Scuseria GE, Robb MA, Cheeseman JR, Zakrzewski VG, Montgomery Jr, JA, Stratmann RE, Burant JC, Dapprich S, Millam JM, Daniels AD, Kudin KN, Strain MC, Farkas O, Tomasi J, Barone V, Cossi M, Cammi R, Mennucci B, Pomelli C, Adamo C, Clifford S, Ochterski J, Petersson GA, Ayala PY, Cui Q, Morokuma K, Malick DK, Rabuck AD, Raghavachari K, Foresman JB, Cioslowski J, Ortiz JV, Stefanov BB, Liu G, Liashenko A, Piskorz P, Komaromi I, Gomperts R, Martin RL, Fox DJ, Keith T, Al-Laham MA, Peng CY, Nanayakkara A, Gonzalez C, Challacombe M, Gill PMW, Johnson B, Chen W, Wong MW, Andres JL, Gonzalez C, Head-Gordon M, Replogle ES, Pople JA (1998) Gaussian Inc , Pittsburgh PA
30. Dunning TH Jr (1989) J Chem Phys 90:1007
31. Kendall RA Jr, Dunning TH Jr, Harrison RJ (1992) J Chem Phys 96:6796
32. Moller C, Plesset MS (1934) Phys Rev 46:618
33. Head-Gordon M, Pople JA, Frisch MJ (1988) Chem Phys Lett 153:503
34. Glendening ED, Reed AE, Carpenter JE, Weinhold F NBO Version 3.1
35. Bader RFW (1990) Atoms in molecules—a quantum theory. Oxford University Press, Oxford
36. Biegler-Köning F, Schönbohm J, Bayles D (2001) J Comput Chem 22:545
37. Biegler-Köning (2000) AIM2000, version 1 0, University of Applied Sciences, Bielefeld, Germany
38. Tarakeshwar P, Choi HS, Lee SJ, Lee JY, Kim KS, Ha TK, Jang JH, Lee JG, Lee H (1999) J Chem Phys 111:5838
39. Díaz-Acosta I, Alvarez-Idaboy JR, Vivier-Bunge A (1999) Int J Chem Kinet 31:29
40. Alvarez-Idaboy J, Mora-Diez N, Vivier-Bunge A (2000) J Am Chem Soc 122:3715
41. Curtiss LA, Frurip DJ, Blander M (1979) J Chem Phys 71:2703
42. Reimers; Watts R, Klein M (1982) Chem Phys 64:95
43. Benson SW (1982) The foundations of chemical kinetics. Krieger, Florida
44. Okuno Y (1997) Chem-Eur J 3:212
45. Alvarez-Idaboy JR, Reyes L, Cruz J (2006) Org Lett 8:1763
46. Bader RFW, Essen H (1984) J Chem Phys 80:1943
47. Kuno M, Hannongbua S, Morokuma K (2003) Chem Phys Lett 380:456
48. Udier-Blagovic M, Tirado-Rives J, Jorgensen WL (2004) J Med Chem 47:2389

49. Nunrium P, Kuno M, Saen-oon S, Hannongbua S (2005) Chem Phys Lett 405:198
50. Cocuzza AJ, Chidester DR, Cordova BC, Jeffrey S, Parsons RL, Bacheler LT, Erickson-Viitanen S, Trainor GL, Ko SS (2001) Bioorg Med Chem Lett 11:1177
51. Högberg M, Sahlberg C, Engelhardt P, Noréen R, Kangasmetsä J, Johansson NG, Öberg B, Vrang L, Zhang H, Sahlberg Bl, Unge T, Lövgren S, Fridborg K, Bäckbro K (1999) J Med Chem 42:4150